

# Terahertz Modulators Based on Silicon P-I-N-Structures in Dielectric Waveguides

V. Grimalsky<sup>\*</sup>, S. Koshevaya, A. Zamudio-Lara, J. Escobedo-Alatorre  
Autonomous University of State Morelos (UAEM), Cuernavaca, ZP 62209, Mor., Mexico

<sup>\*</sup>E-mail: v\_grim@yahoo.com

(Received 24 March 2011; accepted 14 June 2011)

**Abstract:** Simulations of the interaction of terahertz (THz) waves with the silicon integrated *p-i-n*-structures in the isolated silicon dielectric waveguides have been done. The modulation of the fundamental almost linearly polarized electromagnetic mode is considered. This modulation is essential in the case of highly doped  $p^{++}$ ,  $n^{++}$  regions, which provide the double injection of electrons and holes into *i*-region. The generalized boundary conditions at the injecting electrodes have been applied in the case of highly doped  $p^{++}$ ,  $n^{++}$  regions. The silicon dielectric waveguides possess the low losses in the regime without the injection. The investigations of the modulation properties of the integrated *p-i-n*-structures in the dielectric waveguides of THz range have demonstrated a possibility to use these structures up to the frequencies  $\leq 8$  THz. The transmission and the modulation of picoseconds electromagnetic monopulses have been demonstrated too.

**Keywords:** Terahertz modulator, Silicon dielectric waveguide, integrated *p-i-n*-structure

**doi:** [10.11906/TST.059-070.2011.06.08](https://doi.org/10.11906/TST.059-070.2011.06.08)

## 1. Introduction

In the past years, much attention has been given to electromagnetic (EM) terahertz (THz) frequency range, 0.1 THz - 10 THz [1]-[11]. In this range it is necessary to use the novel electrodynamics structures, because the traditional metallic waveguides possess the high losses; therefore, it is better to utilize the dielectric waveguides (DW) [12]-[15]. Below, the isolated DW is considered, where the wave guiding rod with the permittivity  $\epsilon_2$  is separated from the metallic base by a dielectric isolation layer ( $\epsilon_1 < \epsilon_2$ ). In isolated DW the losses are smaller, when comparing with the image DW without a dielectric layer. It is possible to fabricate an isolated DW from highly resistive silicon with SiO<sub>2</sub> isolation layer, see below in Fig. 1. As an effective control device, the integrated *p-i-n*-structures also made of silicon can be used [16].

In quasi-optic modulators the integrated structures are placed in the cross-section of the oversized metallic waveguide [16], and the thickness of the structure cannot be smaller than 50  $\mu\text{m}$ . This is connected with a reduction of its durability. In silicon DW it is possible to fabricate the structures directly within the waveguide or to insert this structure into the aperture within the waveguide core. There is no problem with the mechanic durability of the modulator in this case. The structures should provide the small losses of EM waves in the regime without the injection and the high modulation degree in an injection regime. But a change of the frequency-dependent effective dielectric permittivity due to injected carriers in THz range is not high as in the millimeter wave range. Moreover, in the millimeter wave range the modulation of the effective permittivity has mainly the imaginary part, whereas in THz range such a modulation includes both real and imaginary parts.

To obtain the higher values of concentrations of the carriers injected into *i*-region of *p-i-n*-structures, it is necessary to use the structures with highly doped  $p^{++}$ ,  $n^{++}$  regions [17]. In the highly doped  $p^{++}$ ,  $n^{++}$  regions the majority carriers become degenerated and the narrowing of the forbidden gap occurs both from the side of the conduction band  $\Delta E_c$  and from the valence band  $\Delta E_v$  [17],[18],[19]. The modification of the boundary conditions for injected carriers at  $p^{++-i}$ ,  $n^{++-i}$  junctions was done in [20], [21].

In the present paper the EM wave modulation in THz range based on the integrated *p-i-n*-structures in the silicon isolated DW is theoretically investigated. For the injection problem, the generalized boundary conditions at  $p^{++-i}$  and  $n^{++-i}$  injecting junctions have been applied. It has been demonstrated that silicon DWs possess relatively low dissipation of EM modes in THz range, whereas the modulation due to *p-i-n*-structures is high up till the frequencies 7 - 8 THz.

## 2. Geometry and Model

In this paper the experience of fabrication and experimental investigation the surface oriented *p-i-n* structures of the following geometry is used [16]. The real structures included the planar structure, which consists of planar periodic metal and *p-i-n* regions with deep injecting junctions. These structures were tested experimentally [16]. Surface oriented silicon integrated *p-i-n*-structures with deep injecting junctions have demonstrated a high efficiency in the whole millimeter wave range as quasi-optical modulators and phase shifters [16].

The integrated surface oriented *p-i-n*-structure is a plate made of highly resistive silicon or another material, where a set of injecting deep  $n^+-i$  and  $p^+-i$  junctions is fabricated on one of its sides, see Fig.1, a.

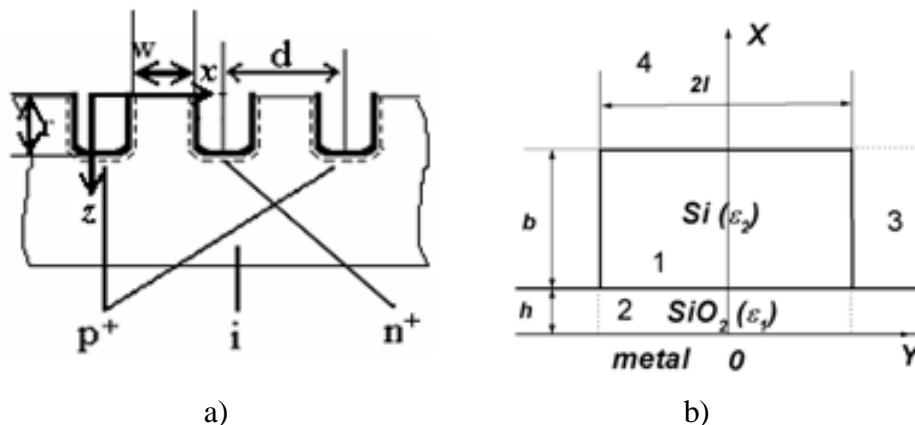


Fig.1 Cross-section of integrated *p-i-n*-structure (a) and silicon isolated DW (b).

These  $p^+-i$  and  $n^+-i$  junctions are “deep” junctions [16] with the depth of doped regions  $r = 10 - 25 \mu m$ . The geometry of the structure is as follows, see Fig.1: the thickness of silicon plate is  $50 - 250 \mu m$ , the width of *i*-region  $w = 10 - 40 \mu m$ , the metallization value  $\gamma = w/d = 0.5; 0.73; 0.8$ , or  $(d-w)/d = 0.1 - 0.3$ . The silicon plate is made of a material having the resistivity  $\rho_0 > 10^3 Ohm \cdot cm$ .

The control of a  $p-i-n$  diode is based on the following phenomenon. Under the action of a control signal, the charge carriers are injected into the  $i$ -region of the diode from the  $p$ - and  $n$ -regions. Thus, the electron-hole plasma is created in  $i$ -region of the diode shielded from the microwave signal. In the absence of a control signal, the microwave power passes through  $i$ -region with small losses. The high-speed time of  $p-i-n$  diode may be shown to increase with a decrease in  $i$ -layer thickness, however, the permitted microwave switch level decreases in this case. This limitation is very important for the volume of the  $p-i-n$  diode. The operation characteristics of microwave modulators based on  $p-i-n$  structures are: the initial losses, the inserted attenuation (decoupling), and the speed of response, the width of the operating frequency range, the control currents, and the controlled amounts of power. All these parameters may be obtained by theoretical and experimental methods [16].

### 3. Modes of Isolated DW

The propagation of modes of the isolated DW has been simulated by means of partial regions, or the Marcatili method, and by the effective dielectric constant method [12]-[15]. The selection of partial regions is given in Fig.1, b. A case  $l > b$  is considered. Generally, all the components of the electric field  $\mathbf{E}$  are present in the fundamental mode  $LP_{11}^x$ . But the dominating component is the vertical one  $E_x$ . The impedance boundary conditions have been used at the metallic surface. It is possible to utilize the approximate calculations by means of partial regions [12], where the electromagnetic field out of the selected partial regions 1,2,3,4 is neglected. For  $LP^x$  modes all the field components can be expressed through the single component of the electric Hertz vector  $\vec{\Pi}^e = \vec{e}_x \Pi$ . The Hertz vector satisfies the Helmholtz equation:

$$\begin{aligned} \Delta \Pi + k_0^2 \varepsilon \Pi &= 0; \quad \Pi \sim \exp(i\omega t); \quad k_0^2 \equiv \frac{\omega^2}{c^2}; \\ E_x &= \omega^2 \varepsilon \Pi + c^2 \frac{\partial^2 \Pi}{\partial x^2}; \quad E_y = c^2 \frac{\partial^2 \Pi}{\partial x \partial y}; \quad E_z = c^2 \frac{\partial^2 \Pi}{\partial x \partial z}; \\ H_x &= 0; \quad H_y = \frac{i\omega \varepsilon}{\mu_0} \frac{\partial \Pi}{\partial z}; \quad H_z = -\frac{i\omega \varepsilon}{\mu_0} \frac{\partial \Pi}{\partial y} \end{aligned} \quad (1)$$

In each partial region the corresponding value of permittivity should be used.

The boundary conditions of the continuity of tangential components of the electromagnetic field are equivalent to:

$$\begin{aligned} x = h, \quad x = h + b: \quad \frac{\partial \Pi}{\partial x} \text{ is} \\ \text{continuous}; \quad y = l: \quad \varepsilon \frac{\partial \Pi}{\partial x} \text{ is continuous} \end{aligned} \quad (2)$$

At the metallic surface  $x = 0$ , the impedance boundary condition is used:

$$E_z = ZH_y, \quad \text{or,} \quad \frac{\partial \Pi}{\partial x} - i\omega \varepsilon_0 \varepsilon \Pi = 0. \quad (3)$$

Here  $Z$  is the surface impedance of the metal. The propagating EM modes are searched as:  $\Pi \sim \exp(i\omega t - ikz)$ . The solutions for the partial regions are:

$$\begin{aligned} \Pi &= (A_1 \cdot \cos(q_x(x-h)) + A_2 \cdot \sin(q_x(x-h))) \cdot \cos(q_y y) \quad - \text{region } 1; \\ \Pi &= (B_1 \cdot \cosh(rx) + B_2 \cdot \sinh(rx)) \cdot \cos(q_y y) \quad - \text{region } 2; \\ \Pi &= (C_1 \cdot \cos(q_x(x-h)) + C_2 \cdot \sin(q_x(x-h))) \cdot \exp(-s(|y|-l)) \quad - \text{region } 3; \\ \Pi &= D \cdot \exp(-p(x-b-h)) \cdot \exp(q_y y) \quad - \text{region } 4. \end{aligned} \quad (4)$$

The transverse wave numbers  $q_x, q_y$  satisfy the following equations:

$$\begin{aligned} &\frac{r}{\varepsilon_1} \left( \tanh(rh) + \frac{i\omega \varepsilon_0 \varepsilon}{r} Z \right) \cdot \left( \frac{q_x}{\varepsilon_2} \cos(q_x b) + p \sin(q_x b) \right) \\ &- \frac{q_x}{\varepsilon_2} \left( 1 + \frac{i\omega \varepsilon_0 \varepsilon}{r} Z \tanh(rh) \right) \cdot \left( \frac{q_x}{\varepsilon_2} \sin(q_x b) - p \cos(q_x b) \right) = 0; \end{aligned} \quad (5)$$

$$q_y \tan(q_y l) - s = 0;$$

$$\text{where } r^2 = k_0^2 (\varepsilon_2 - \varepsilon_1) - q_x^2, \quad s^2 = k_0^2 (\varepsilon_2 - 1) - q_y^2.$$

First of all, it is necessary to solve Eqs. (5) for  $q_x, q_y$ , then one can get the longitudinal wave number  $k$  of the mode as:

$$k^2 = k_0^2 \varepsilon_2 - q_x^2 - q_y^2. \quad (6)$$

The approximation of this simulation method is valid, when the inequalities are satisfied:  $k_0^2 \varepsilon_2 \gg q_x^2, q_y^2$ , or, equivalently, when  $|E_y| \ll |E_x|$ . But namely this situation is interesting for practical applications, because the injecting junctions are oriented along the axis OY, as shown in Fig.1, a, b, and the reflection of the fundamental mode of DW is small in the regime without injection.

The working frequency band is limited from below by the frequency where the maximum value of  $|E_y|$  component of the fundamental mode is 10% from the maximum value of its  $|E_x|$  component. At higher frequencies, it is assumed the excitation of higher modes is suppressed. A typical dispersion relation of silicon DW ( $\varepsilon_1 = 11.7, \varepsilon_2 = 3.9$ ) is given in Fig.2.

The used sizes of DW are: the thickness of the core is  $b = 0.2 \text{ cm}$ , the thickness of the isolator is  $h = 0.05 \text{ cm}$ , the width is  $2l = 1 \text{ cm}$ . The metallic substrate is copper. At frequencies  $f \leq 50 \text{ GHz}$  the waveguide dispersion is essential, whereas at higher frequencies  $f > 100 \text{ GHz}$  the dispersion relation is practically a straight line  $k = k_0(\varepsilon_2)^{1/2}$  and the wave dispersion is absent. The wave dissipation at  $f > 50 \text{ GHz}$  is small:  $\text{Im}(k) < 0.1 \text{ cm}^{-1}$ . When the thickness of the isolator is finite  $h \neq 0$ , the fundamental mode possesses the cut-off. But practically the frequency region for DW is

determined by localization of the fundamental mode, or, in another words, by the condition  $|E_x| \gg |E_y|$ .

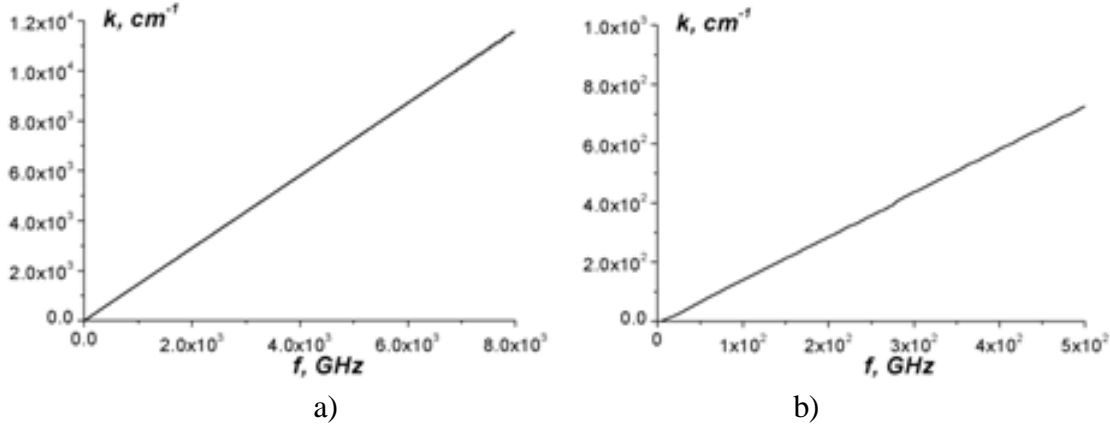


Fig.2 The wave dispersion of the fundamental mode of DW (a). More detailed one at lower frequencies (b).

#### 4. Injection Problem

The basic assumptions are: the  $p^{++}$ - $i$ ,  $n^{++}$ - $i$  junctions are abrupt; the simplest parabolic approximation for the density of states  $N_v$ ,  $N_c$  both in  $p^{++}$ ,  $n^{++}$ , and  $i$ - regions; neglecting the recombination at the contacts. The recombination at the contacts can decrease the concentrations of injected carriers on 20 - 40 % when the nonlinearity of boundary conditions is not essential. But when the concentrations are higher than  $2 \times 10^{17} \text{ cm}^{-3}$ , the nonlinearity of boundary conditions becomes dominating, as our simulations have demonstrated.

The injection problem is simulated within a framework of the ambipolar diffusion equation added by the boundary conditions at  $n^{++}$ - $i$  and  $p^{++}$ - $i$  junctions and on free surfaces [16],[20],[21]:

$$\begin{aligned}
 \frac{\partial n}{\partial t} - D \left( \frac{\partial^2 n}{\partial x^2} + \frac{\partial^2 n}{\partial z^2} \right) + \frac{n}{T_l} &= 0; \\
 2D_p (\bar{\kappa} \nabla n) - \left( 1 + \frac{D_p}{D_n} \right) \frac{D_{np^{++}}}{w_{p^+}} n(p^{++}) &= -\frac{j_0}{q}; \\
 2D_n (\bar{\kappa} \nabla n) - \left( 1 + \frac{D_n}{D_p} \right) \frac{D_{pn^{++}}}{w_{n^+}} p(n^{++}) &= -\frac{j_0}{q}; \\
 (\bar{\kappa} \nabla n) - \gamma_s n &= 0
 \end{aligned} \tag{7}$$

Here  $n(x,z,t)$  is the concentration of injected carriers;  $D_{n,p}$ ,  $D = 2D_n D_p / (D_n + D_p)$  are the diffusion coefficients of electrons, holes, and the ambipolar diffusion in  $i$ -region, correspondingly;  $T_l$  is the lifetime of carriers there. The value  $N_{d,a}$  are the concentrations of donors and acceptors in  $n^{++}$  and  $p^{++}$  regions; the value  $w_{n^+,p^+}$  are the thicknesses of these regions, the value  $D_{np^{++}}$  is the diffusion coefficient for the minority carriers (electrons) within the  $p^{++}$  region; and OZ-axis is directed perpendicularly to the surface of structure and coincides with the axis of DW, OX -axis is perpendicular to OZ-axis (see Fig. 1). The unit vector  $\kappa(x,z)$  is normal to  $p^{++}$ - $i$ ,  $n^{++}$ - $i$  interfaces or to a free surface and is directed into the  $i$ -region. The parameter  $\gamma_s$  is the recombination

coefficient at free surfaces. A distribution of the electric current density  $j_0$  is assumed as uniform along the surface of the injecting junctions. The last fact is confirmed by the calculations of the distributions of electric potential within the  $i$ -region.

The value of  $n(p^{++})$  is determined by the following equation (analogously for  $p(n^{++})$ ) [20], [21]:

$$n(p^{++}) = \frac{n^2}{N_v} \exp\left(\frac{\varphi_{Fp}}{\varphi_T} + \frac{\Delta\varphi_c}{\varphi_T}\right) \quad (8)$$

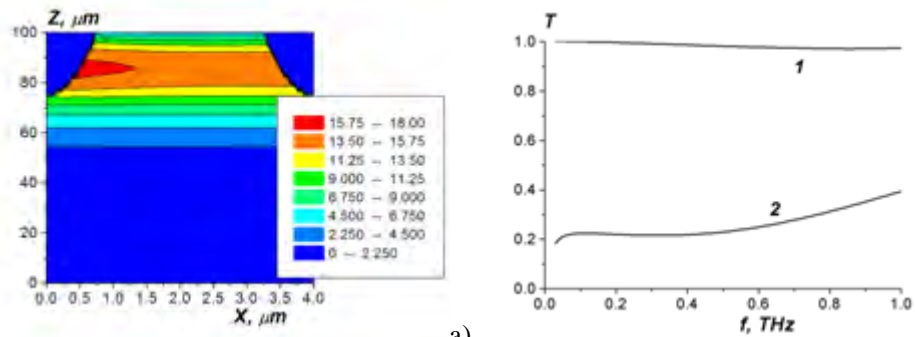
Here  $\varphi_{Fp}$ ,  $\varphi_{Fn}$  are the quasi-Fermi levels, which are measured in Volts,  $\varphi_{Fp,n} = F_{p,n}/q$ ,  $\Delta\varphi_{v,c} = \Delta E_{v,c}/q$ ,  $\varphi_T = k_B T_e / q = 0.026$  V at the room temperature  $T_e = 300$  K. Note that the narrowing of the forbidden gap leads to increase of the density of the current due to the minority carriers and to decrease of the injection efficiency, whereas the smaller diffusion coefficients of the minority carriers in the highly doped regions [17],[19],[22] partially compensate this decreasing. It was calculated also the values of concentrations of minority carriers when a more accurate approximation for the density of the states within the highly doped regions is used. The results of the simulations are practically the same as in the simple parabolic approximation.

## 5. Numerical Simulations

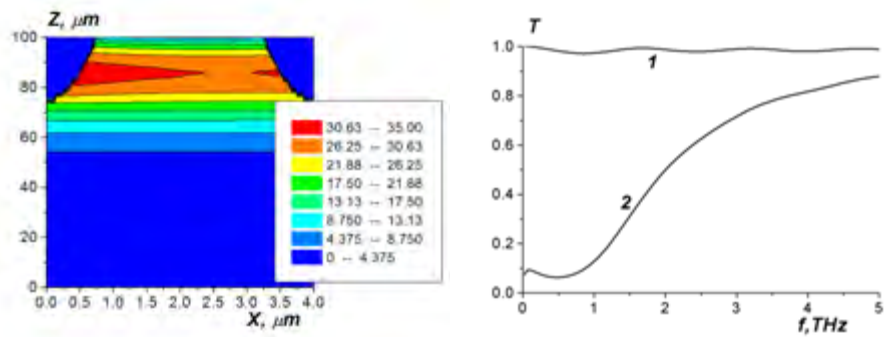
Under high injection levels the boundary conditions are nonlinear due to the current of the minority carriers in the highly doped regions. The numerical simulations show that in the structures with the deep junctions an influence of the surface recombination is unessential, when the depth of the junctions is  $r \geq 15 \mu m$ . The injection takes place mostly into the region between the junctions, and the transverse distribution of the concentration of the injected carriers is uniform. Moreover, within DW it is possible to get the thickness of the structure along the OZ-axis equal to the depth of the injecting electrodes and to provide the double injection between the electrodes exactly.

The following parameters are used in the simulations: the distance between the centers of electrodes is  $d = 4 - 8 \mu m$ , the thickness of  $i$ -layer is  $w = 1.5 - 5 \mu m$ , the depth of the injecting electrodes is  $r = 15 - 25 \mu m$ ,  $w_{n+}/L_{n+} = w_{p+}/L_{p+} = 0.05$ . The lifetime of the carriers in the  $i$ -region is  $T_l = 10 \mu s$ , the doping levels are  $10^{18} - 10^{20} cm^{-3}$ . The density of the injection current is  $j_0 = 100 - 3000 A/cm^2$ . Under the parameters pointed above, it is possible to achieve the concentrations of the injected carriers up to  $n \sim (5 - 8) \times 10^{17} cm^{-3}$ .

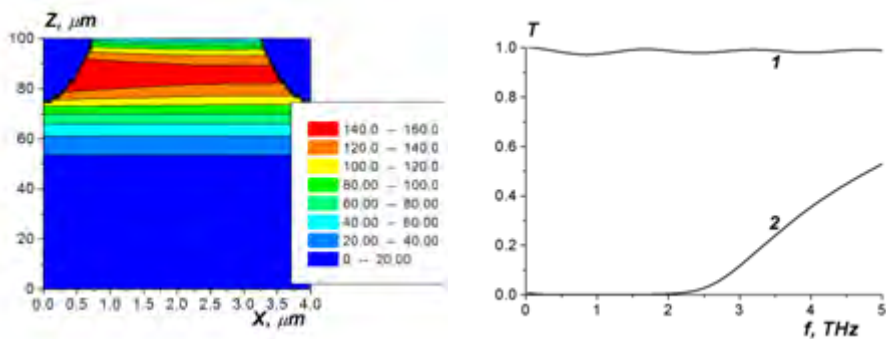
The distributions of the concentrations of the injected carriers are given in Fig. 3, left parts. The depth of the injecting junctions is  $r = 25 \mu m$  here, the  $p^{++}$  region is on the left side. The nonlinearity is a limiting factor for the further increase of the injection at  $j_0 > 1000 A/cm^2$ . Under the concentrations  $n > 10^{18} cm^{-3}$  the Auger recombination processes may be important, and the ambipolar diffusion equation within the  $i$ -region becomes nonlinear. The time of establishing can be estimated as  $\sim 0.3w^2/D$ ; and it is about 3 - 10 ns here. Note that the decrease of the sizes of the injecting junctions leads to decrease of the concentrations of the injected carriers, due to the nonlinearity of the boundary conditions (the thicknesses of highly doped layers  $w_{p+}$ ,  $w_{n+}$  are in denominators, see Eqs. (1)). Therefore, there exists some optimum distance between the junctions of the structure to produce the maximum injection level.



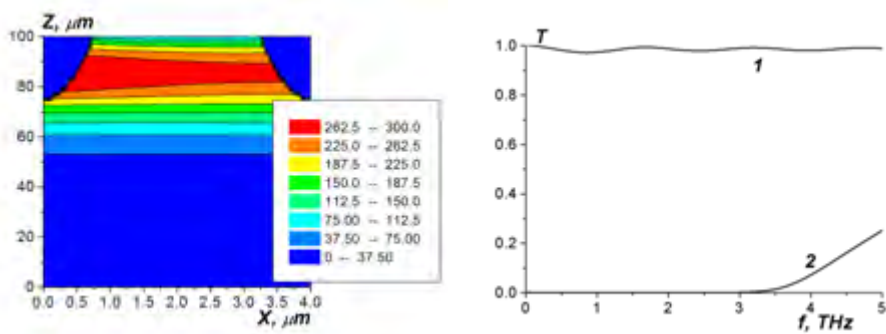
a)



b)



c)



d)

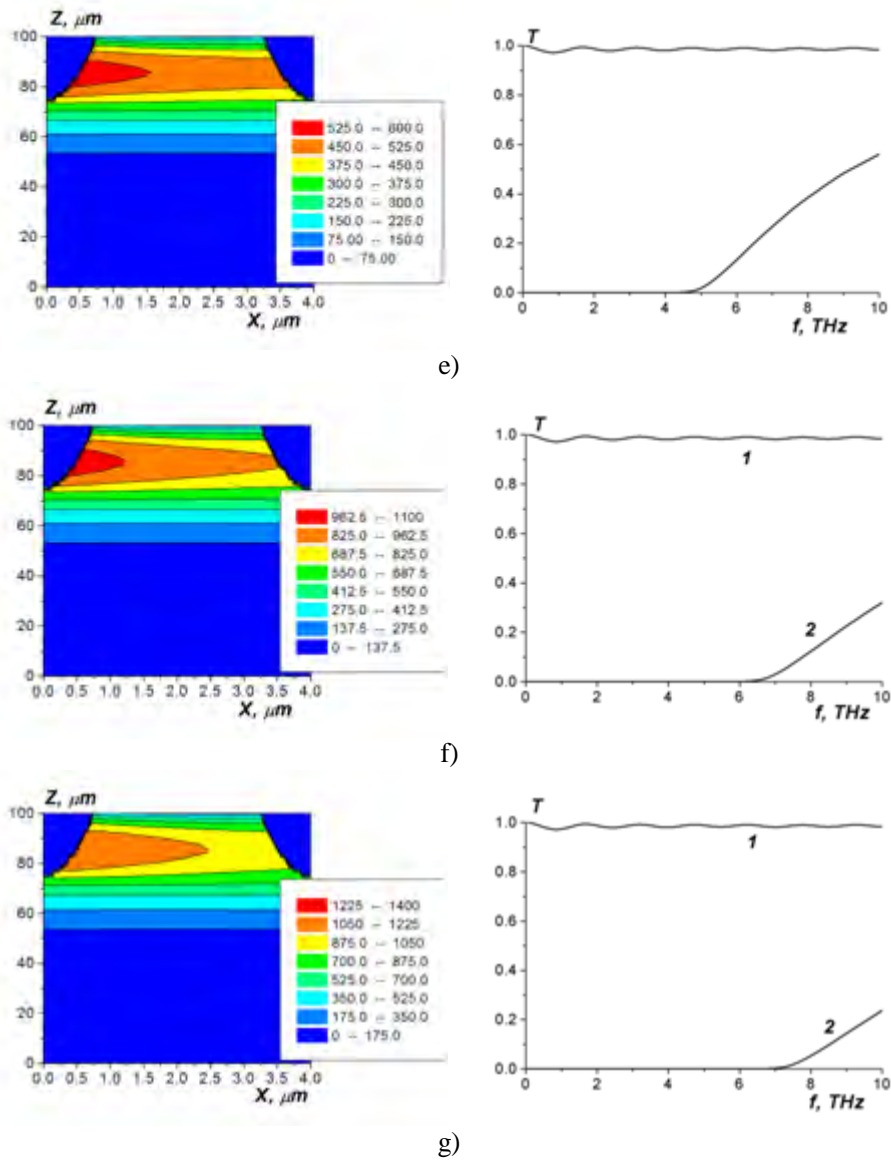


Fig.3 Distribution of injected carriers ( $10^{15} \text{ cm}^{-3}$  units), left parts; transmission coefficients without injection (line 1) and with it (line 2), right parts. The doping concentrations of  $n^{++}$ ,  $p^{++}$  junctions are  $N_d = N_a = 10^{20} \text{ cm}^{-3}$ , the densities of current are:  $j_0 = 50 \text{ A/cm}^2$  (part a);  $j_0 = 100 \text{ A/cm}^2$  (part b);  $j_0 = 500 \text{ A/cm}^2$  (part c);  $j_0 = 1000 \text{ A/cm}^2$  (part d);  $j_0 = 2000 \text{ A/cm}^2$  (part e);  $j_0 = 4000 \text{ A/cm}^2$  (part f);  $j_0 = 5000 \text{ A/cm}^2$  (part g).

The modulation of the fundamental EM  $LP_{11}^x$  mode, which is mostly  $x$ -polarized, has been investigated. There is no necessity to use the clarifying layers here, in comparison with a quasi-optical modulator [16],[20], where the propagation of EM beams in the oversize metallic waveguide was considered.

The used parameters of DW are: the width is  $2l = 0.2\text{-}1 \text{ cm}$ , the thickness of the silicon core is  $b = 0.05 - 0.4 \text{ cm}$ , the thickness of the isolator  $\text{SiO}_2$  layer is  $h = 0.01\text{-}0.05 \text{ cm}$  ( $h < b < l$ ). The following expression for effective (averaged) dielectric permittivity in  $X$ - and  $Z$ -directions has been used [23]:

$$\begin{aligned}\varepsilon_{eff}(z) &= d \cdot \left( \int_0^d \varepsilon^{-1}(x, z, \omega) dx \right)^{-1}; \\ \varepsilon &= \varepsilon_l \left( 1 - \frac{\omega_{pe}^2}{\omega(\omega - i\nu_e)} - \frac{\omega_{ph}^2}{\omega(\omega - i\nu_h)} \right); \\ \omega_{pe,h}^2 &= \frac{q^2 n(x, z)}{\varepsilon_0 \varepsilon_l m_{e,h}}\end{aligned}\quad (9)$$

Here  $\varepsilon_l$  is the lattice part of the relative dielectric permittivity ( $\varepsilon_l \equiv \varepsilon_2 = 11.7$  for Si); the parameter  $\varepsilon_0$  is the electric constant; the values  $\nu_{e,h}$  are the collision frequencies of electrons and holes;  $m_{e,h}$  are the effective masses of the carriers [17],[22];  $\omega \equiv 2\pi f$ ,  $\omega_{pe,h}$  are the plasma frequencies. The incident EM wave is mainly polarized along OX-axis, and the averaging takes place for the inverse value of the complex dielectric permittivity  $\varepsilon^{-1}$  [23]. The waveguide modes mainly polarized along OY-axis are reflected from the structure completely because for the component  $E_y$  it is necessary to average the complex dielectric permittivity  $\varepsilon(x, z, \omega)$ , which is high in the metallic regions. Thus, the *p-i-n*-structure can be represented as the part of the DW where the effective permittivity differs from the permittivity of the isolating silicon. In the regime without injection, such a permittivity is 10 - 15% higher than one of the silicon. In the injection regime, it is essentially complex and its absolute value increases.

The propagation of the localized fundamental  $LP_x^{11}$  mode is considered, the ratio  $|E_y|/|E_x|$  is smaller than 0.1 within the waveguide as our simulations have demonstrated. Therefore, in the regime without injection the EM mode can pass through the *p-i-n*-structure, and the reflection coefficient is <10% higher than for the plane wave at the same frequency.

The results of the calculations of the transmission coefficients  $T$  for the intensity of EM waves are presented in Fig. 3, right parts. The used sizes of DW are: the thickness of the core is  $b = 0.2$  cm, the thickness of the isolator layer is  $h = 0.05$  cm, the width is  $2l = 1$  cm. To get the good modulation is the whole millimeter wave range  $f = 30 - 300$  GHz; it is sufficient to use the moderate values of the injection current density  $j_0 \leq 50$  A/cm<sup>2</sup>, see Fig. 3. The values of  $j_0$  should be higher:  $j_0 \geq 200$  A/cm<sup>2</sup> for the modulation in THz range. It is possible to obtain the good modulation properties in DWs with Si structures up till the frequencies  $f \leq 7 - 8$  THz. Namely, in the regime with the injection of the carriers the EM wave transmission coefficients  $T$  are smaller than 0.25. The wider operation frequency range has been achieved here when compared with the quasi-optical modulator in the oversize metallic waveguide. The problem of the heating of the structure is not so serious, as compared with quasi-optical modulators because there is a good mechanical contact.

A principal problem in THz range is the generation and the transmission of short monopulses, i.e., the EM pulses that possess extremely wide frequency band and have the durations of about 1 - 10 ps. Because it is possible to obtain the wide operation frequency range both in the regime without injection and with injection, the propagation of short monopulses through the DW has been considered too. In Fig. 4 the dependencies of  $E_x$  component of the monopulse on the time  $t$  are given. The distances of DW along OZ-axis are 0.1 - 0.5 cm.

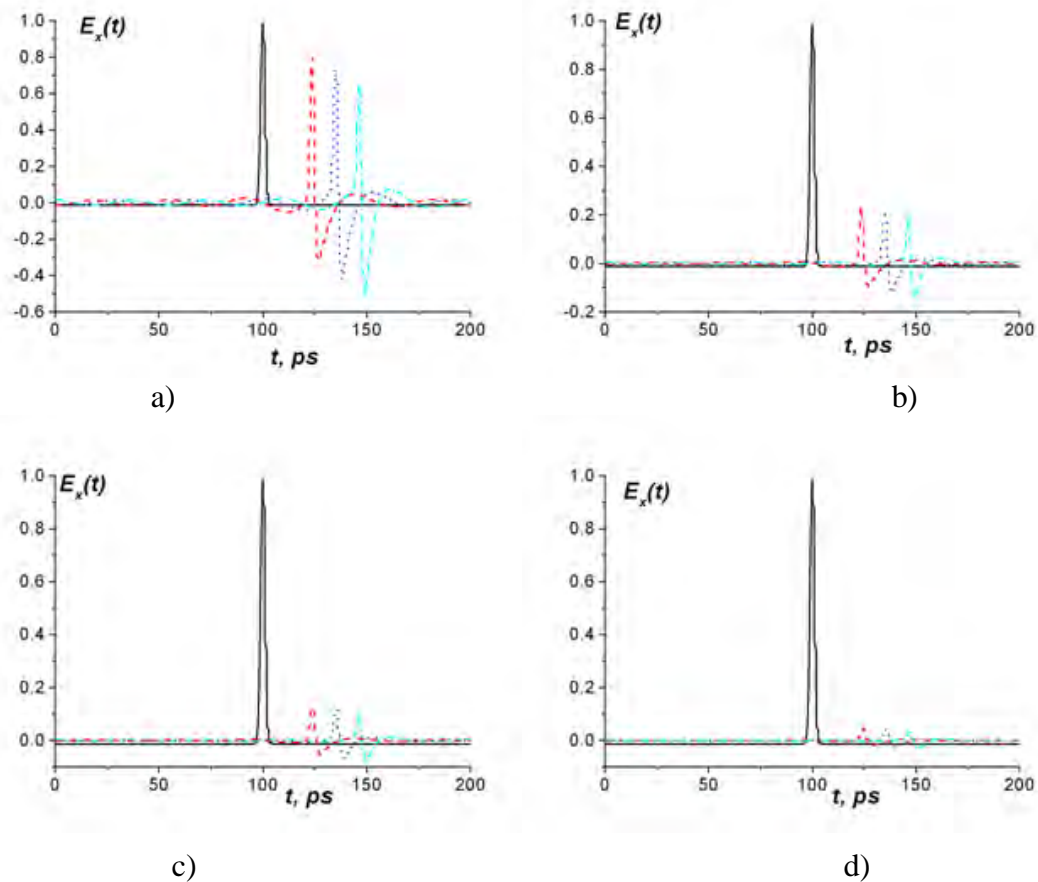


Fig.4 Transmission of the monopulse through DW with  $p-i-n$ -structure. The doping levels are  $N_d = N_a = 10^{20} \text{ cm}^{-3}$ . Solid line is the initial pulse, dash line is the transmitted pulse at the distance  $L_z = 0.2 \text{ cm}$  from  $p-i-n$ -structure, dot line is one at  $L_z = 0.3 \text{ cm}$ , dash-dot line is the pulse at  $L_z = 0.4 \text{ cm}$ . Part a) is without injection, part b) is at  $j_0 = 100 \text{ A/cm}^2$ , part c) is at  $j_0 = 200 \text{ A/cm}^2$ , part d) is at  $j_0 = 500 \text{ A/cm}^2$ .

One can see that there is a possibility to transfer the pulses of picosecond durations through the DWs without essential distortion up till the distances of 0.3 cm and to modulate them. The waveguide dispersion leads to distortion of monopulses at longer distances.

## 6. Conclusion

The simulation of the modulation properties of integrated silicon  $p-i-n$ -structures in the dielectric waveguides of THz range has demonstrated a possibility to use these structures up to the frequencies  $\approx 8 \text{ THz}$ .

The deep  $p^{++-i}$  and  $n^{++-i}$  injecting junctions with high doping demonstrate a good injection and are useful for the obtaining of higher concentrations of injected carriers within the  $i$ -region. The propagation and the modulation of vertically polarized fundamental  $LP_{11}^x$  electromagnetic mode of the dielectric waveguides has been considered. Because the value of the horizontal electric field component  $E_y$  of the fundamental mode is small, this mode passes through the

structure without reflection in the regime without injection. The silicon integrated  $p-i-n$ -structures with deep  $p^{++}$ ,  $n^{++}$  regions can be used as effective modulators in THz range. There is no necessity to use any matching layers in the dielectric waveguides, and the operation frequency range can be wide. Dielectric waveguides also can be used for the transmission and the modulation of electromagnetic monopulses of picosecond durations.

## Acknowledgement

This work was partially supported by SEP-CONACyT (Mexico).

## References

- [1] P.Siegel, "Terahertz technology", *IEEE Trans. MTT*, 50(3), 910 – 928, (2002).
- [2] P.Siegel, "THz technology in biology and medicine", *IEEE Trans. MTT*, 52(10), 2438 – 2447, (2004).
- [3] F.Rodriguez-Morales, K.S.Yngvesson, R.Zannoni e.a., "Development of integrated HEB/MMIC receivers for near-range terahertz imaging", *IEEE Trans. MTT*, 54(6), 2301-2311, (2006).
- [4] Yun-Shik Lee, "Principles of terahertz science and technology", *Springer, N.Y.*, (2009).
- [5] M. Shur, "Terahertz technology: devices and applications", *Proceedings of ESSDERC*, Grenoble, France, (2005).
- [6] M. Tonouchi, "Galore new applications of terahertz science and technology". *Terahertz Science and Technology*, 2(3), 90-101, (2009).
- [7] M. Mukherjee, S. Banerjee, and J. P. Banerjee, "Dynamic characteristics of III-V and IV-IV semiconductor based transit time devices in the terahertz regime: a comparative analysis", *Terahertz Science and Technology*, 3(3), 97-109, (2010).
- [8] V. Dobrovolsky, F. Sizov, V. Zabudsky, N. Momot, "Mm/sub-mm bolometer based on electron heating in narrow-gap semiconductor", *Terahertz Science and Technology*, 3(1), 33-54, (2010).
- [9] H. Zhan, R. Mendis, and D.M. Mittleman, "Terahertz energy confinement in finite-width parallel-plate waveguides", *Terahertz Science and Technology*, 2(4), 144-149, (2009).
- [10] Y. Hao, L.-A. Yang, and J.-C. Zhang, "GaN-based semiconductor devices for terahertz technology", *Terahertz Science and Technology*, 1(2), 51-64, (2008).
- [11] V.G. Bozhkov, "Semiconductor detectors, mixers, and frequency multipliers for the terahertz band", *Radiophys. Quant. Electr.*, 46(4) 631-656, (2003).
- [12] D.Marcuse, "Theory of dielectric optical waveguides", *Academic Press*, Boston, (1990).
- [13] S.F.Mahmoud, "Electromagnetic waveguides", *Peter Pelegrinus*, London, (1991).
- [14] T.Rozzi and M.Mongiardo, "Open electromagnetic waveguides", *IEE Press*, London, (1997).
- [15] C. Yeh and F. I. Shimabukuro, "The essence of dielectric waveguides", *Springer*, Berlin, (2008).
- [16] S. Koshevaya, E. Gutierrez-D., M. Hayakawa e.a., "Interaction of powerful electromagnetic waves with integrated P-I-N-structures", *Jap. J. Appl. Phys.*, 37(5), 643-646, (1998).

- [17] S.Sze and Kwok K.Ng, "Physics of Semiconductor Devices", *Wiley-Interscience*, N.Y., (2006).
- [18] Web Site <http://www.ioffe.ru/SVA/NSM/> (New semiconductor materials. Characteristics and properties).
- [19] B. Shklovskii and A. Efros, "Electronic properties of doped semiconductors", *Springer*, Berlin, (1984).
- [20] V. Grimalsky, S. Koshevaya, D. Chillon-E., and J. Escobedo-A., "Integrated silicon *p-i-n*-structures for modulation in terahertz range with highly doped P<sup>++</sup>, N<sup>++</sup> regions", *Proceedings of 26<sup>th</sup> Intl. IEEE Conference on Microelectronics (MIEL)*, Nis, Serbia, 263 – 266, (2008).
- [21] V.V. Grimalsky, S.V. Koshevaya, and M. Tecpoyotl-T., "Integrated silicon *p-i-n* structures with highly doped  $p^{++}$ ,  $n^{++}$  regions for modulation in terahertz frequency band", *Radioelectronics and Communications Systems*, 53(6), 309-313, (2010).
- [22] F. Schwierz and J. Liou, "Modern microwave transistors", *Wiley-Interscience*, N.Y., (2003).
- [23] R. Vitlina and A. Dykhne, "Reflection of electromagnetic waves from a surface with a low relief", *Soviet Physics – JETP*, 72(6), 983-990, (1991).